Cation−π Interactions in Ligand Recognition by Serotonergic (5-HT_{3A}) and Nicotinic Acetylcholine Receptors: The Anomalous Binding Properties of Nicotine†

Darren L. Beene,‡ Gabriel S. Brandt,‡ Wenge Zhong,‡,|| Niki M. Zacharias,‡ Henry A. Lester,§ and Dennis A. Dougherty*,‡

Divisions of Chemistry and Chemical Engineering and Biology, California Institute of Technology, Pasadena, California 91125

Received April 8, 2002; Revised Manuscript Received May 31, 2002

ABSTRACT: A series of tryptophan analogues has been introduced into the binding site regions of two ion channels, the ligand-gated nicotinic acetylcholine and serotonin 5-HT_{3A} receptors, using unnatural amino acid mutagenesis and heterologous expression in *Xenopus* oocytes. A cation−π interaction between serotonin and Trp183 of the serotonin channel 5-HT_{3A}R is identified for the first time, precisely locating the ligand-binding site of this receptor. The energetic contribution of the observed cation−π interaction between a tryptophan and the primary ammonium ion of serotonin is estimated to be approximately 4 kcal/mol, while the comparable interaction with the quaternary ammonium of acetylcholine is approximately 2 kcal/mol. The binding mode of nicotine to the nicotinic receptor of mouse muscle is examined by the same technique and found to differ significantly from that of the natural agonist, acetylcholine.

Synaptic transmission is largely mediated by neurotransmitters and the receptors that bind them. At the core of this process is the selective recognition and binding of a small molecule by its protein host. Despite the pharmacological and clinical significance of compounds that modulate synaptic signaling, the chemical basis of neurotransmitter binding has been difficult to determine. High-resolution structural data on neuroreceptors with bound agonists are only just becoming available (*1*−*4*), and functional data are still needed to distinguish which agonist−receptor interactions are mechanistically significant.

Nearly all neurotransmitters contain a cationic center, and a common strategy for biological recognition of cations is the cation−π interaction, the stabilizing interaction between a cation and the negative electrostatic potential on the face of an aromatic ring (*5*, *6*). We have recently introduced a technique for the in situ identification of cation−π binding sites (*7*). This technique relies on nonsense suppression methodology for site-specific introduction of an unnatural amino acid into a functioning receptor expressed in a living cell (*8*−*11*). In the first application of the technique, a series of fluorinated Trp derivatives was introduced at various positions in the binding region of the nicotinic acetylcholine receptor (nAChR).[1] At Trp 149 of the α subunit, the EC_{50} of ACh for receptor activation was strongly correlated to the degree of fluorination. These findings, and others obtained by nonsense suppression, were subsequently confirmed by the recently reported crystal structure of an ACh binding protein (AChBP) (*3*). This protein shares significant structural and sequence homology with the nAChR ligand-binding domain. (Figures 1 and 2) The crystal structure of AChBP revealed that the binding site is a box of aromatic

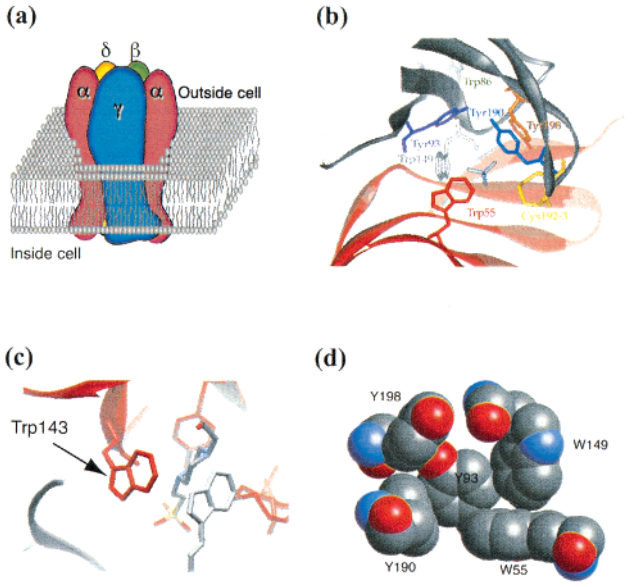

FIGURE 1: Several views of the nicotinic acetylcholine receptor (nAChR). (a) A schematic of the receptor, indicating the arrangement of five subunits around a central pore. The extracellular ligand-binding domain is shown, along with the pore-forming transmembrane domain. (b) Details of the binding site illustrating the prevalence of aromatic residues. The coordinates come from X-ray diffraction of an ACh binding protein with extremely high homology to nAChR. (c) Diffraction data from AChBP showing a HEPES molecule from the crystallization buffer bound to the face of Trp143, the homologue of muscle nAChR Trp149 and 5-HT_{3A}R Trp183. (d) The "aromatic box" comprising the nAChR active site, based on AChBP coordinates.

† This work was supported by NIH Grants NS-34407 and NS-11756 and Boehringer-Ingelheim.

* Corresponding author. Telephone: (626) 395−6089. Fax: (626) 564−9297. E-mail: dad@igor.caltech.edu.

‡ Division of Chemistry and Chemical Engineering, Caltech.

§ Division of Biology, Caltech.

|| Current address: Amgen, Inc., One Amgen Center Drive, MS 29-2-C, Thousand Oaks, CA 91320.

[1] Abbreviations: nAChR, nicotinic acetylcholine receptor; 5-HT_{3A}R, 5-hydroxytryptamine type 3A receptor; ACh, acetylcholine; 5-HT, 5-hydroxytryptamine (serotonin); AChBP, acetylcholine binding protein; HEPES, *N*-(2-hydroxyethyl)piperazine-*N*′-(2-ethanesulfonic acid); 5-HTQ, *N*,*N*,*N*-trimethyl-5-hydroxytryptamine; norACh, 2-dimethyl aminoethyl acetate; TMA, tetramethylammonium.

10.1021/bi020266d CCC: $22.00
Published on Web 07/19/2002

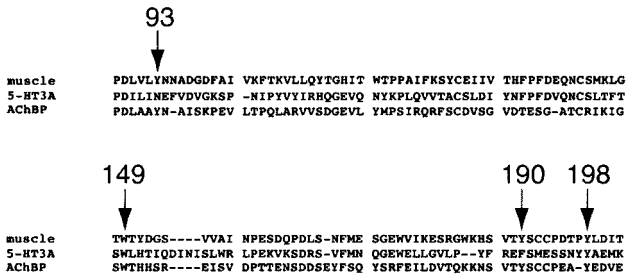

FIGURE 2: Sequence alignment of muscle nAChRα, 5-HT$_{3A}$R, and AChBP. The residues that comprise the aromatic box are indicated with arrows, with the exception of the Trp residue contributed by the interfacial subunit, which is conserved among all members of the nAChR receptor family and which is γ55 or δ57 in muscle nAChR and α90 in 5-HT$_{3A}$R.

residues, including the critical Trp α149 (Figure 1). Electron density corresponding to a molecule of HEPES was seen in this box with its ammonium center bound to Trp α149, as expected for a cation−π interaction.

The nAChR belongs to a superfamily of ligand-gated ion channels that includes the 5-hydroxytryptamine-3 (5-HT$_3$R), glycine, and γ-aminobutyric acid receptors (*12*−*14*). These receptors are composed of five homologous subunits arranged around a central pore. The tertiary structure of these subunits is modular: the agonist binding site is located in the extracellular N-terminal domains, and the ion channel is located in the transmembrane domains (Figure 1).

In the present work, we extend the application of the unnatural amino acid mutagenesis technique to the serotonin-gated ion channel, 5-HT$_{3A}$R. We also further evaluate cation−π interactions at the nAChR, considering nicotine and several other agonists. These studies involving unnatural amino acids generate two major findings. The first is that 5-HT$_{3A}$R Trp 183, which aligns with Trp α149 in the nAChR, binds the primary ammonium of serotonin (5-hydroxytryptamine, or 5-HT) via a cation−π interaction. The second is that, in the muscle nAChR, nicotine does not apparently experience a strong cation−π interaction with Trp α149. The first result is consistent with the idea that the binding site of the serotonin channel is highly homologous to that of nAChR. The second result, however, is surprising in light of accepted pharmacophore models for the nicotinic receptor. Because of questions raised by these results, a series of both serotonin and nicotine derivatives were analyzed with the goal of delineating differences and establishing similarities between the two binding sites.

RESULTS

Unnatural amino acids were incorporated into the 5-HT$_{3A}$R and nAChR using in vivo nonsense suppression methods, and mutant receptors were evaluated electrophysiologically (*8*−*11*). The structures and electrostatic potential surfaces of the side chains of the unnatural amino acids utilized are presented in Figure 3. Electrostatic potential surfaces provide a useful guide for evaluating the cation−π binding ability of an aromatic ring (*15*, *16*). These surfaces show how electron-withdrawing groups such as cyano and fluoro substantially weaken the cation−π interaction. The agonists used in these studies are presented in Figure 4, along with their electrostatic potential surfaces. Note that the energy scales of the electrostatic potential plots are very different

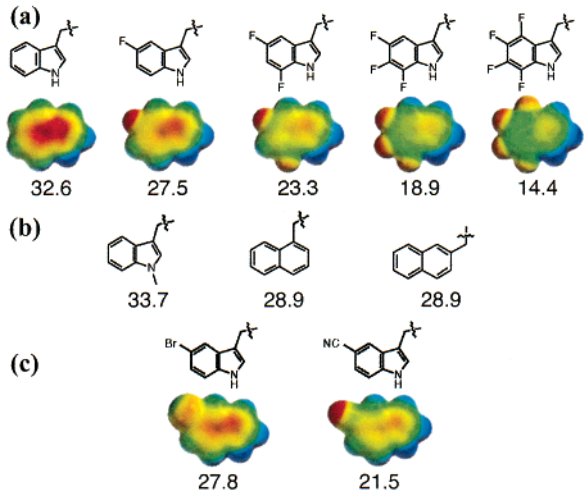

FIGURE 3: Side chains introduced in place of binding site Trp residues. (a) The series of fluorinated Trp analogues, with the gas-phase cation-π binding energy of fluoroindoles (HF 6-31G**) in kcal/mol. (b) Trp analogues without the indole nitrogen hydrogen bond donation ability, along with calculated cation−π binding energy. (c) Trp analogues for screening Trp sites for electrostatic interactions, with calculated cation−π binding ability. AM1 electrostatic surfaces are colored according to an energy scale corresponding to ± 25 kcal/mol, where blue is positive and red is negative.

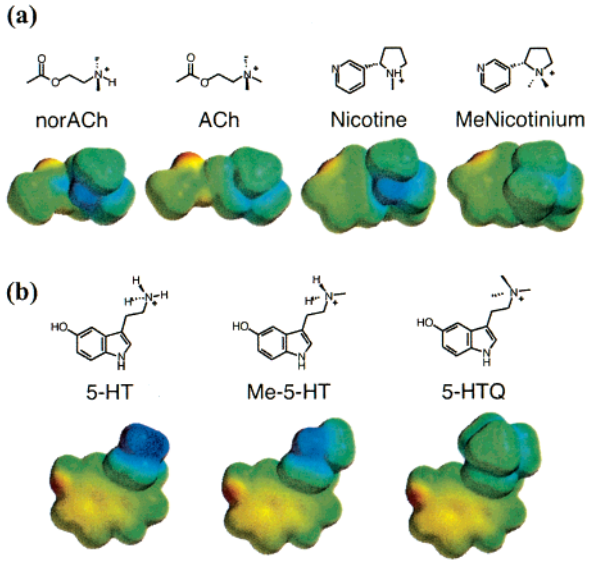

FIGURE 4: Agonists utilized in this study (a) nAChR agonists, with AM1 electrostatic surfaces calculated using Spartan showing the overall geometrical similarity of the structurally distinct nicotinoid and cholinergic agonists. (b) 5-HT$_{3A}$R agonists, with AM1 electrostatic surfaces showing the varying charge density around the nitrogen center. Electrostatic surfaces correspond to an energy range of −5 to +160 kcal/mol, where blue is positive and red is negative.

for Figures 3 and 4. For the side chains, the scale is ± 25 kcal/mol, such that red is negative and blue is positive electrostatic potential. However, the structures of Figure 4 are all cations, and so the energy range is −5 to 160 kcal/mol. For a cation, the surface is positive everywhere; red simply represents relatively less positive, and blue represents relatively more positive.

When studying weak agonists and/or receptors with diminished binding capability, we and others have found it necessary to introduce a Leu-to-Ser mutation at a site known as 9′ in the second transmembrane region of the receptor

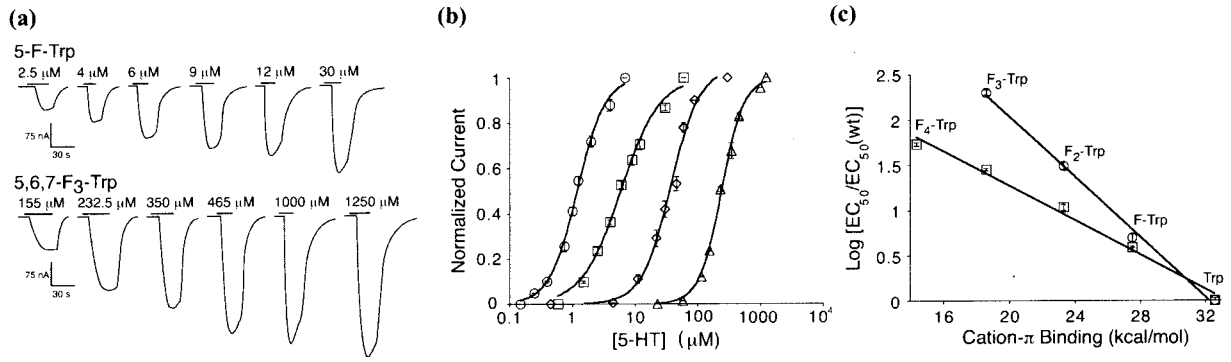

FIGURE 5: Electrophysiological analysis of 5-HT. (a) Representative voltage-clamp current traces for oocytes expressing suppressed 5-HT_{3A}R's. Bars represent application of 5-HT. (b) 5-HT dose−response relations and fits to the Hill equation for 5-HT_{3A}R's suppressed with Trp (○), F-Trp (□), F_2-Trp (◇), and F_3-Trp (△) at position 183. (c) Fluorination plot (log[EC_{50}/EC_{50} (wt)] versus calculated cation−π binding ability for the series of fluorinated Trp derivatives) for 5-HT (○) at the 5-HT_{3A}R and ACh (□) at the nAChR. 5-HT data fit the line $y = 5.37 - 0.17x$ and ACh data fit the line $y = 3.2 - 0.096x$. The correlation for both linear fits is $r = 0.99$.

(*17*, *18*). This site is almost 50 Å from the binding site, and previous work has shown that each L9′S mutation lowers EC_{50} by a factor of roughly 10, with multiple L9′S mutations having an additive effect. Results from earlier studies and data reported below clearly demonstrate that trends in EC_{50} values are not perturbed by L9′S mutations (*18*). For the present study, we have used receptors that contain one or two L9′S mutations, as noted in the tables and figure captions.

Finally, it should be noted that the quantity we report here, EC_{50}, is not a binding constant, but a composite of equilibria for both binding and gating (*19*). An advantage of EC_{50} is that it represents a *functional* assay; all mutant receptors reported here are fully functioning ligand-gated ion channels. This alleviates concerns that the mutations introduced cause a massive structural reorganization of the receptor. Because the subtle mutations we make are in the region of the agonist binding site, and the presumptive gate of the ion channel is almost 50 Å away, we assume variations in EC_{50} for the series of unnatural residues reflect differential agonist-binding ability, and that the gating equilibrium is not substantially perturbed.

5-HT_{3A}R Studies. Two subunits, A and B, have been identified for the 5-HT_3R (*20*, *21*). Only the 5-HT_{3A}R when expressed alone in heterologous expression systems forms functional homomeric receptors, and the 5-HT_3R studies presented here were carried out using homomeric 5-HT_{3A} receptors. Previous work has shown that the homomeric and heteromeric (A and B) receptors share a common pharmacology while differing somewhat in biophysical properties, such as conduction, kinetics, and desensitization characteristics (*22*).

Position 183 in the 5-HT_{3A}R. Because of the well-established effect of fluorine substitution in modulating the cation−π interaction, a series of fluorinated Trp derivatives (5-F-Trp, 5,7-F_2-Trp, 5,6,7-F_3-Trp, and 4,5,6,7-F_4-Trp) was incorporated at position 183, the analogue of Trp α149. Whole-cell currents and fits to the Hill equation, presented in Figure 5a−b, demonstrate that these receptors display the functional hallmarks of 5-HT_3R's—desensitization to prolonged agonist exposure and Hill coefficients around 2. The EC_{50} values for the wild type and the mutants are given in Table 1. A clear trend can be seen from the data. Each additional fluorine produces an increase in EC_{50}. Attempts to record dose−response relations from the incorporation of 4,5,6,7-F_4-Trp at 183 were unsuccessful, because this mutant required highly elevated concentrations of 5-HT, concentrations at which the agonist becomes an effective open channel-blocker.

Table 1: Dose−Response Data for 5-HT_{3A}R with Unnatural Amino Acids

	residue	EC_{50} (μM)[a]
	W183	
5-HT	Trp	1.2 ± 0.1
	F-Trp	6.0 ± 0.5
	F_2-Trp	37 ± 3
	F_3-Trp	244 ± 8
N-Me-5-HT	Trp	1.8 ± 0.1
	F-Trp	2.7 ± 0.2
	F_2-Trp	23 ± 3
	F_3-Trp	368 ± 12
5-HTQ	Trp	1.1 ± 0.1
	F-Trp	1.6 ± 0.1
	F_2-Trp	13 ± 1
	F_3-Trp	284 ± 19
5-HT	1-Np-Ala	30 ± 2
	2-Np-Ala	32 ± 2
	N-Me-Trp	26 ± 2
	W90	
5-HT	Trp	1.2 ± 0.1
	F_4-Trp	1.1 ± 0.0

[a] EC_{50} ± standard error of the mean.

As in previous work on the nAChR, our measure for the cation−π binding ability of the fluorinated Trp derivatives is the calculated binding energy (kcal/mol) of a generic probe cation (Na^+) to the corresponding substituted indole (*7*, *15*). This provides a convenient way to express the clear trend in the dose−response data in a more quantitative way. Extensive studies of the cation−π interaction establish that *trends* in cation−π binding ability across a series of aromatics are independent of the identity of the cation, justifying the use of a simple probe ion. To also place the dose−response data for the channel on an energy scale, the logarithmic ratio of EC_{50} for mutants to EC_{50} for wild type is used. We will refer to such representations as "fluorination plots." A plot of this ratio versus cation−π binding ability for Trp183 reveals a compelling relationship (Figure 5c). Over a range of greater than 2 orders of magnitude in EC_{50}, there is a linear correlation between log(EC_{50}) and the cation−π binding ability of the side chains. We feel this provides substantial evidence that Trp 183 binds 5-HT through a cation−π

interaction arising from van der Waals contact between the agonist ammonium group and the indole side chain.

Along with modulating the cation−π interaction, fluorination also increases the ability of a Trp analogue to donate a hydrogen bond (*23*, *24*). Therefore, an alternative interpretation of the above results would be that the hydrogen bonding ability of the NH of the indole side chain of Trp 183 decreases receptor activation, and that fluorinated Trp analogues decrease activation by increasing the hydrogen bond strength. This hypothesis suggests that EC_{50} would be decreased by side chains that decrease hydrogen bond strength but remain isosteric with Trp. To test this hypothesis, a series of Trp analogues lacking a hydrogen bond donor at the nitrogen position of indole was incorporated at position 183 (Figure 3b). The EC_{50} values for 2-Np-Ala, 1-Np-Ala, and N-Me-Trp were 32, 30, and 26 μM, respectively (Table 1). The increased EC_{50} is opposite to the prediction of the hydrogen bond hypothesis. Thus, it appears that modulation of hydrogen bonding ability does not explain the increase in EC_{50} in response to fluorination.

Position 90 in the 5-HT_{3A}R. An important question is whether the dramatic fluorination effect seen at position 183 in the 5-HT_{3A}R is unique to this site, as was observed for Trp α149 in the nAChR. In principle, the cation could interact simultaneously with several sides of the aromatic box. On the basis of sequence alignment and the AChBP structure, Trp 90 likely forms part of the binding site in the 5-HT_{3A}R. Thus, 4,5,6,7-F_4-Trp was incorporated at position 90. The EC_{50} value of this mutant was almost identical to wild type—1.1 and 1.2 μM—respectively, indicating that Trp 183 defines the cation−π binding site in the 5-HT_{3A}R.

N-Me-5-HT and 5-HTQ at the 5-HT_{3A}R. Dose−response relations were recorded for the secondary serotonin analogue *N*-methyl-5-hydroxytryptamine (N-Me-5-HT) and the quaternary derivative *N*,*N*,*N*-trimethyl-5-hydroxytryptamine (5-HTQ) with the fluoro-Trp series at position 183 (Figure 4b). The results for these experiments are presented in Table 1. Mono or tris methylation at the ammonium center of 5-HT has a minimal effect on EC_{50}; both agonists are comparable to the natural ligand serotonin. At position 183 in the 5-HT_{3A}R, as with 5-HT itself, each additional fluorine substituent produces an increase in EC_{50}, indicating a significant cation−π interaction with the ammonium centers in both N-Me-5-HT and 5-HTQ.

Effect of Agonist Alkylation State at the nAChR. As a complement to the studies of N-Me-5-HT and 5-HTQ at the 5-HT_{3A}R, we studied the behavior of the tertiary ACh analogue, 2-dimethyl aminoethyl acetate (noracetylcholine, or norACh) and the "simplified" quaternary ACh analogue tetramethylammonium (TMA) at the nAChR (Figure 4a). While TMA is a very low-potency agonist (Table 2), it does appear to experience a cation−π interaction with Trp α149 similar to that seen for ACh. Only data up to F_3-Trp are available, because, as with other agonists studied, channel blockade by the agonist becomes a serious problem at the high concentrations necessary to activate the receptor with F_4-Trp at α149. Clearly, though, progressive fluorination leads to a steady increase in EC_{50} as seen with ACh.

The results for norACh highlight a significant difference between the 5-HT_{3A}R and the nAChR. While substantial variation in the alkylation state of 5-HT has no significant effect on potency, simply removing one methyl group from the quaternary ammonium of ACh to produce norACh leads to vastly inferior potency (Table 2). The EC_{50} for norACh is comparable to that of TMA. The fluorination data for norACh are not completely straightforward (Table 2). While monofluorination shows a 7-fold increase, comparable to ACh, di- and trifluorination show only modest increases and tetrafluorination leads to a *decrease* in EC_{50}.

Table 2: Dose−Response Data for nAChR with Unnatural Amino Acids

	residue	EC_{50} (μM)[a]
	W149	
ACh	Trp	1.2 ± 0.0
β L9′S	F-Trp	4.7 ± 0.1
	F_2-Trp	13 ± 1
	F_3-Trp	34 ± 1
	F_4-Trp	65 ± 3
TMA	Trp	48 ± 2
β,δ L9′S	F-Trp	155 ± 4
	F_2-Trp	313 ± 8
	F_3-Trp	789 ± 23
norACh	Trp	23 ± 6
β,γ L9′S	F-Trp	161 ± 9
	F_2-Trp	225 ± 28
	F_3-Trp	327 ± 18
	F_4-Trp	152 ± 4
nicotine	Trp	45 ± 1
β L9′S	F-Trp	130 ± 5
	F_2-Trp	172 ± 6
	F_3-Trp	188 ± 11
	F_4-Trp	136 ± 5
nicotine	Trp	1.3 ± 0.3
β,γ L9′S	F-Trp	4.2 ± 0.7
	F_2-Trp	5.4 ± 0.5
	F_3-Trp	12 ± 1
	F_4-Trp	11 ± 1
Menicotinium	Trp	0.8 ± 0.1
β,γ L9′S	F-Trp	4.2 ± 0.4
	F_2-Trp	5.7 ± 0.7
	F_3-Trp	3.3 ± 0.4
	F_4-Trp	4.6 ± 1.0
	γ55/δ57	
nicotine	CN-Trp	1.4 ± 0.2
α_2 L9′S	Br-Trp	3.0 ± 0.4

[a] EC_{50} ± standard error of the mean.

Nicotine Dose−Response to F_n-Trp Series at α149 in Muscle nAChR. Nicotine is, of course, an important agonist of the nAChR, and all pharmacophore models for this drug and related compounds align the protonated pyrrolidine nitrogen with the quaternary ammonium of ACh (*25*−*29*). To evaluate this model, we have studied nicotine's potency with the series of fluorinated Trp derivatives at position α149 of the nAChR. The results are shown in Table 2 and Figure 6. Dose−response relations were collected for receptors with one (β subunit) or two ($\beta\gamma$ subunits) L9′S mutations. The results are similar in each case. If a single fluorine is added to the tryptophan ring by incorporating F-Trp at position α149, the EC_{50} increases almost 3-fold, which is comparable to the 4-fold increase observed with ACh. However, further fluorination does not lead to a significant further increase in EC_{50}. Figure 6b shows a fluorination plot for nAChR with a single L9′S mutation in the β subunit. Clearly, the progressive rise in EC_{50} seen with ACh and other agonists is not seen with nicotine.

Nicotine Dose−Response to Trp Analogues at γ55/δ57 in Muscle nAChR. The lack of a strong response to fluorination at Trp α149 by nicotine indicates that it does

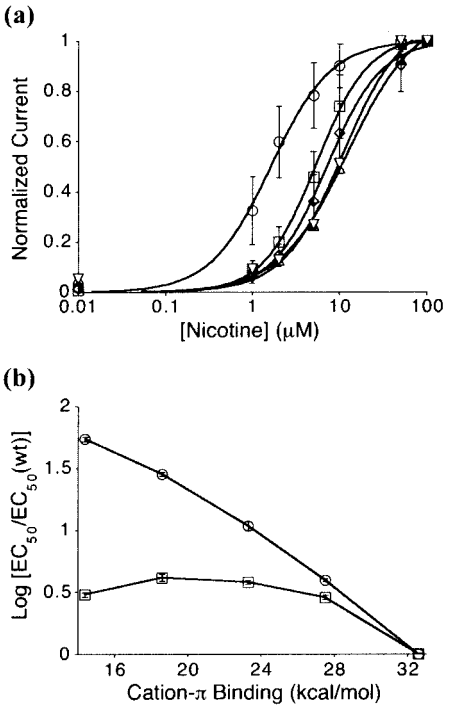

FIGURE 6: Electrophysiological analysis of nicotine. (a) Nicotine dose−response relations for β L9′S nAChR suppressed with Trp (○), F-Trp (□), F_2-Trp (◇), F_3-Trp (△), and F_4-Trp (▽) at α149. (b) Fluorination plot for ACh (○) and nicotine (□) at the nAChR.

not experience a significant cation−π interaction with this residue. This suggests the possibility that another aromatic residue in the binding site might form a cation−π interaction with nicotine. On the basis of the crystal structure of AChBP, an appealing candidate is Trp γ55/δ57, which is adjacent to Trp α149 in the binding site. We therefore evaluated the γ55/δ57 pair using, instead of fluorination, the alternative comparison of 5-CN-Trp vs 5-Br-Trp. As discussed previously, this nearly isosteric pair provides a useful qualitative indicator of a cation−π interaction, since the cyano group is much more strongly deactivating than the bromo (Figure 3c). For example, at α149 with ACh as the agonist, the ratio of EC_{50} values for 5-CN-Trp/5-Br-Trp is 57 (*7*). As shown in Table 2, the ratio 5-CN-Trp/5-Br-Trp is approximately 0.5 for nicotine at the γ55/δ57 position. This is not at all consistent with a cation−π interaction between nicotine and this tryptophan.

N-Methyl-Nicotinium Dose−Response to F_n-Trp Series at nAChR α149. Both ACh and TMA show a progressive increase in EC_{50} with fluorination, while nicotine does not. This suggests that a quaternary ammonium ion may be essential to see this effect in nAChR binding. To test this possibility, we evaluated the quaternary analogue *N*-methyl-nicotinium in the $\beta\gamma$ L9′S nAChR. As shown in Table 2, the EC_{50} for *N*-methyl-nicotinium at wild-type receptors is similar to that of nicotine. In addition, *N*-methyl-nicotinium behaves quite similarly to nicotine in the fluorination plot. Thus, the unusual behavior of nicotine is not due to the lack of a quaternary ammonium group.

Studies of Agonist Efficacy. The EC_{50} for a receptor is a composite measurement, comprising multiple elementary steps. Even in the simplest two-state model of channel opening, agonist binding to the closed channel is followed by a conformational change to an open channel state. Since the dose−response measurement does not distinguish between these two steps, experiments were undertaken to determine whether binding or channel gating accounted for the observed alterations in EC_{50} in response to increasing Trp fluorination. The efficacy of a compound on a ligand-gated ion channel is reflected in the maximal current passed at saturating agonist concentration under given electrophysiological conditions (*19*, *30*). Relative efficacies of all drugs were determined in ND96 medium in oocytes clamped at a membrane potential of −80 mV at a concentration five times the EC_{50} of the compound. For the nAChR agonists considered here, there was no statistical difference in efficacy among them. Nor was the relative efficacy ever observed to differ in receptors containing fluorinated Trp analogues. The process of channel gating is a complicated one and is postulated to involve numerous elementary steps for the nAChR. Thus, it is overly simplistic to conclude from these efficacy experiments that the effects observed are due exclusively to binding (*31*). However, the fact that all compounds tested exhibit a similar ability to initiate the conformational changes associated with channel opening suggests the large effects that we see on potency most likely arise from effects on agonist binding.

DISCUSSION

The agonist response of a ligand-gated channel testifies to the organizing power of weak, noncovalent interactions. As the neurotransmitter approaches the much larger receptor, it must not be lured in by sites whose charge, shape, and hydrophobicity resemble the intended binding site. Instead, the molecule diffuses within the synaptic cleft and is drawn exactly to the appropriate location to trigger channel opening. In the case of the nicotinic acetylcholine receptor, we have previously proposed a unique role for Trp149 in the α subunit in the binding of the natural agonist, acetylcholine (*7*). On the basis of subtle alterations of the electrostatic surface of the side chain at this position, we concluded that it participates in a strong cation−π interaction with the quaternary ammonium center of ACh. More recent structural work from other labs on AChBP has confirmed this conclusion (*3*). In the work presented here, we extend this technique to a related serotonin receptor, the 5-HT_{3A}R. In addition, we expand the scope of our study at both the nAChR and 5-HT_{3A}R to consider in greater detail the nature of the interaction between agonist and receptor. Homology between the 5-HT_{3A}R, the alpha subunit of the muscle nAChR, and AChBP is significant, with strong conservation of the tryptophan residues making up two sides of the ligand-binding site box. In addition, two of the three tyrosine residues seen in the nAChR and AChBP are aromatic amino acids in 5-HT_{3A}R (Figure 2) (*32*).

The introduction of a series of fluorinated Trp analogues at position 183 of the mouse 5-HT_{3A}R provides clear evidence for a cation−π interaction between this residue and serotonin, as suggested by earlier site-directed mutagenesis studies (*33*). This interaction appears to be unique to Trp183. Substitution of the fluorinated Trp series at Trp 90, also in the binding site region, causes no significant effects. We thus conclude that both the nAChR and the 5-HT_{3A}R make use of a single potent cation−π interaction in recognizing the ammonium centers of their respective agonists.

Interestingly, the slope of the plot relating EC_{50} to calculated cation−π binding energy (the "fluorination plot") is visibly different for ACh binding to nAChR than serotonin binding to the 5-HT_{3A}R. Inspection of Figure 5c shows that the serotonin slope is markedly steeper. We interpret this to mean that the strength of the cation−π interaction between the agonist and the relevant tryptophan is greater when serotonin is the agonist than when ACh is the agonist. This result is consistent with expectations based on electrostatics (*34*). As shown in Figure 4, the smaller, primary ammonium center of serotonin presents a more focused positive charge than the quaternary center of ACh. Given the strong electrostatic component of the cation−π interaction, smaller ions are expected to show a stronger interaction.

The data for ACh and serotonin also provide one way to address a long-standing issue in molecular recognition: what is the strength of a cation−π interaction? From Figure 3a, it may be observed that the surface of F_4-Trp is essentially electrostatically neutral. Thus, a comparison of F_4-Trp and Trp provides a measure of the *electrostatic component* of the cation−π interaction. The F_4-Trp/Trp ratio reflects the energy cost of removing the attractive electrostatics but maintaining the residue, as if the Trp were replaced by a hydrophobic residue of the same shape. This new residue maintains most van der Waals and dispersion interactions but cannot experience a cation−π interaction. For ACh, the F_4-Trp/Trp ratio is 54. For serotonin, the F_4-Trp EC_{50} value is obtained by extrapolation of the line in Figure 5c, which leads to a F_4-Trp/Trp ratio of 836. If these are viewed as ratios of binding constants, then the implied energetics of a cation−π interaction are 2.4 and 4.0 kcal/mol, respectively, for ACh and serotonin. These are consistent with other estimates of the magnitude of the cation−π interaction (*6*), and further establish that this noncovalent binding force is comparable to or stronger than any other individual force considered in biological recognition.

In an effort to probe the molecular recognition properties of these receptors further, we have studied the effects of varying the alkylation state of the cationic center of the agonist. In such studies, a clear distinction emerges between the 5-HT_{3A}R and the nAChR. At the serotonin receptor, the monoalkylated agonist N-Me-5-HT and the quaternary agonist 5-HTQ show essentially the same EC_{50} as the natural agonist 5-HT. This suggests that the 5-HT_{3A}R agonist binding site is fairly tolerant, accommodating the much bulkier 5-HTQ with no loss in potency. These two unnatural agonists respond to fluorination much like the natural agonist serotonin, although the perfect linear trend of Figure 5c is not reproduced. We hesitate to provide an extensive interpretation of this subtle distinction, in which multiple variables, including both the agonist and the protein, are being changed. Clearly, though, a strong cation−π interaction to Trp 183 is involved with all of these agonists.

The nAChR behaves quite differently from the 5-HT_{3A}R in this regard. First, the change from ACh to norACh leads to a very large increase in EC_{50}. Simply removing one methyl group from ACh produces a very low-potency agonist. In fact, norACh is comparable in potency to tetramethylammonium (TMA), which lacks several moieties of the ACh molecule. Interestingly, the quaternary TMA, although a very low-potency agonist, does show a fluorination trend that is similar to that of ACh (Table 2). The norACh fluorination trend is less well-behaved, with a large increase for F-Trp, then minimal further effects for F_2-Trp and F_3-Trp, followed by a downturn at F_4-Trp (Table 2). While this suggests some kind of cation−π interaction for the norACh agonist, more subtle factors may also be operative for this low-potency, non-native agonist. Clearly, the nAChR is much more sensitive to alterations in the region of Trp α149 than the 5-HT_{3A}R is to comparable changes with the aligning Trp 183.

This leaves the case of nicotine, an obviously important agonist of the nAChR. Before discussing our results, a few general comments are in order. The receptor we have studied here is the muscle-type receptor, the isoform found at the neuromuscular junction in the peripheral nervous system. Nicotine is a full agonist at this receptor, but, as shown in Table 2, nicotine is not an especially potent agonist at the muscle receptor. The behavioral and addictive effects of nicotine arise exclusively from effects on the *neuronal* nAChRs (*35*, *36*). These receptors are expressed widely in the central nervous system (*37*, *38*). While the overall architecture of neuronal nAChR is no doubt the same as the muscle type described here, the neuronal receptors are comprised of different combinations of α and β (non-α) subunits. There are many variants of each subunit, but they are highly homologous to the muscle subunits, and all the residues discussed here are conserved in the neuronal receptors (*12*). At present, at least 10 α and 4 β forms are known, termed α_{1-10} and β_{1-4} (α_1 and β_1 are the muscle forms; all the rest are neuronal). Nicotine addiction is thought to depend partially on receptors formed from α_4 and β_2 subunits (stoichiometry unknown) and perhaps receptors involving α_7 (*39*−*41*). While we believe our findings are clearly relevant to the pharmacology of nicotine, it must be remembered that subtle variations could arise in comparable studies of the neuronal receptors.

The fluorination plot for nicotine is shown in Figure 6b. In light of our findings for ACh versus norACh, we also studied N-Me-nicotinium, in which the pyrrolidine nitrogen has been quaternarized. Interestingly, these two nicotinoid agonists are similar, both in potency and in their fluorination plots. The nicotine fluorination plot has the shallowest slope of any we have seen at either the nAChR or the 5-HT_{3A}R. After a relatively small jump in EC_{50} for F-Trp, only very small changes in EC_{50} are seen upon further fluorination of Trp α149.

At present, we feel the most reasonable interpretation of this finding is that there is not a strong cation−π interaction between nicotine and Trp α149 of the muscle-type nAChR. Further work on the neuronal receptors is in progress to more thoroughly test this view. Of course, an obvious possibility is that nicotine makes a cation−π interaction with one of the other aromatics that form the "aromatic box" of the nAChR binding site. A sensible candidate is γ55/δ57, the other conserved Trp in the agonist binding site. This residue has been implicated in nicotine binding by photoaffinity labeling studies from the Cohen group (*42*, *43*). As a probe of this site, we studied the pair 5-CN-Trp/5-Br-Trp. We have shown previously that this nearly isosteric pair can provide a good qualitative indication of a cation−π interaction, since the cyano group is much more strongly deactivating than the bromo. The pair differ by a factor of 57 for ACh at Trp α149 (*7*). However, no significant effect is seen at γ55/δ57

with nicotine (or ACh) as the agonist, ruling out this site for a cation−π interaction with nicotine at the muscle receptor.

The conclusion that nicotine does not bind to the muscle nAChR via a cation−π interaction with tryptophan residues in the aromatic box has implications for existing pharmacophore models of the nAChR. All current pharmacophore models align the quaternary ammonium of ACh with the protonated tertiary amine of nicotine (*25*−*29*). It seems an unavoidable conclusion that such a model requires a cation−π interaction between the cationic center of nicotine and Trp α149, but it is not clear that one exists. The data with norACh suggest that the nAChR is quite sensitive to variations in agonist structure at the cationic center; much more so than the 5-HT_{3A}R. As nicotine analogues are assuming a greater prominence for drug leads in a variety of important diseases, some caution in applying the standard pharmacophore model seems to be in order.

CONCLUSIONS

In earlier work, we have shown that the nonsense suppression methodology provides a powerful tool for evaluating drug−receptor interactions. In particular, fluorination plots can clearly identify a specific cation−π interaction between an agonist and its receptor. Here, we build upon those findings in several ways.

A clear cation−π interaction between serotonin and Trp 183 of the 5-HT_{3A}R is established. A measure of the magnitude of the electrostatic component of the cation−π interaction is provided. We find it to be worth ∼2 kcal/mol for ACh at the nAChR and ∼4 kcal/mol for serotonin at the 5-HT_{3A}R. Studies of other agonists highlight the differences between the two homologous receptors, the nAChR and the 5-HT_{3A}R. The latter is relatively tolerant of changes at the cationic center and maintains a cation−π interaction, while the nAChR seems quite sensitive to changes in the nature of the cationic center of the agonist. Finally, studies of the binding of nicotine to the muscle nAChR suggest that present pharmacophore models may require revision. Work on the neuronal nAChR will be required to further explore this issue.

METHODS

Electrophysiology. Stage VI oocytes of *Xenopus laevis* were harvested according to approved procedures. Recordings were made 24−72 h postinjection in standard two-electrode voltage clamp mode. Oocytes were superfused with calcium-free ND96 solution, as previously reported (*7*). Nicotinic agonists were either synthesized as described earlier (*N*-methyl-nicotinium) (*44*), purchased from Sigma/Adrich/RBI ([−]-nicotine tartrate) or Acros Organics (the tertiary ACh analogue, 2-dimethyl aminoethyl acetate). Serotonin and its analogues were purchased from Sigma/Adrich/RBI. All drugs were prepared in sterile ddi water for dilution into calcium-free ND96. Dose−response data were obtained for a minimum of eight concentrations of agonists for a minimum of three different cells. Curves were fit to the Hill equation to determine EC_{50} and Hill coefficient.

Unnatural Amino Acid Suppression. Synthetic amino acids were conjugated to the dinucleotide dCA and ligated to truncated 74 nt tRNA as described (*8*). Deprotection of charged tRNA was carried out by photolysis immediately prior to co-injection with mRNA, in the manner described (*7*, *45*). Typically, 25 ng of tRNA were injected per oocyte along with mRNA in a total volume of 50 nL/cell. mRNA was prepared by in vitro runoff transcription using the Ambion mMagic mMessage kit. Mutation to insert the *amber* stop codon at the site of interest was carried out by standard means and was verified by sequencing through both strands. For nAChR suppression, a total of 4.0 ng of mRNA was injected in the subunit ratio of 10:1:1:1 α:β:γ:δ. In many cases, one or more subunits contained a L9′S mutation, as discussed above. Mouse muscle embryonic nAChR in the pAMV vector was used, as reported previously. For suppression in homomeric 5-HT_{3A}R, 5.0 ng of mRNA was injected. Mouse 5-HT_{3A}R was used in all cases, in the pAMV vector. Negative and positive controls for suppression were performed in the following way. As a negative control, truncated 74 nt tRNA or truncated tRNA ligated to dCA was co-injected with mRNA in the same manner as fully charged tRNA. At the positions studied here, no current was ever observed from these negative controls. The positive control involved wild-type recovery by co-injection with 74 nt tRNA ligated to dCA-Trp. In all cases, the dose−response was indistinguishable from injection of wild-type mRNA alone.

REFERENCES

1. Armstrong, N., and Gouaux, E. (2000) *Neuron 28*, 165−181.
2. Mayer, M. L., Olson, R., and Gouaux, E. (2001) *J. Mol. Biol. 311*, 815−836.
3. Brejc, K., van Dijk, W. J., Klaassen, R. V., Schuurmans, M., van Der Oost, J., Smit, A. B., and Sixma, T. K. (2001) *Nature 411*, 269−276.
4. Miyazawa, A., Fujiyoshi, Y., Stowell, M., and Unwin, N. (1999) *J. Mol. Biol. 288*, 765−786.
5. Dougherty, D. A. (1996) *Science 271*, 163−168.
6. Ma, J. C., and Dougherty, D. A. (1997) *Chem. Rev. 97*, 1303−1324.
7. Zhong, W. G., Gallivan, J. P., Zhang, Y. N., Li, L. T., Lester, H. A., and Dougherty, D. A. (1998) *Proc. Natl. Acad. Sci. U.S.A. 95*, 12088−12093.
8. Nowak, M. W., Gallivan, J. P., Silverman, S. K., Labarca, C. G., Dougherty, D. A., and Lester, H. A. (1998) *Methods Enzymol. 293*, 504−529.
9. Thorson, J. S., Cornish, V. W., Barrett, J. E., Cload, S. T., Yano, T., and Schultz, P. G. (1998) *Methods Mol. Biol. Protein Syn. Methods Protocols 77*, 43−73.
10. Gilmore, M. A., Steward, L. E., and Chamberlin, A. R. (1999) *Top. Curr. Chem. 202*, 77−99.
11. Sisido, M., and Hohsaka, T. (1999) *Bull. Chem. Soc. Jpn. 72*, 1409−1425.
12. Corringer, P. J., Le Novere, N., and Changeux, J. P. (2000) *Annu. Rev. Pharmacol. Toxicol. 40*, 431−458.
13. Hucho, F., and Weise, C. (2001) *Angew. Chem., Int. Ed. 40*, 3100−3116.
14. Jackson, M. B., and Yakel, J. L. (1995) *Annu. Rev. Physiol. 57*, 447−468.
15. Mecozzi, S., West, A. P., and Dougherty, D. A. (1996) *J. Am. Chem. Soc. 118*, 2307−2308.
16. Mecozzi, S., West, A. P., and Dougherty, D. A. (1996) *Proc. Natl. Acad. Sci. U.S.A. 93*, 10566−10571.
17. Labarca, C., Nowak, M. W., Zhang, H., Tang, L., Deshpande, P., and Lester, H. A. (1995) *Nature 376*, 514−516.
18. Kearney, P. C., Nowak, M. W., Zhong, W., Silverman, S. K., Lester, H. A., and Dougherty, D. A. (1996) *Mol. Pharmacol. 50*, 1401−12.
19. Kenakin, T. (1999) *Trends Pharmacol. Sci. 20*, 400−405.
20. Maricq, A. V., Peterson, A. S., Brake, A. J., Myers, R. M., and Julius, D. (1991) *Science 254*, 432−437.
21. Davies, P. A., Pistis, M., Hanna, M. C., Peters, J. A., Lambert, J. J., Hales, T. G., and Kirkness, E. F. (1999) *Nature 397*, 359−363.
22. Brady, C. A., Stanford, I. M., Ali, I., Lin, L., Williams, J. M., Dubin, A. E., Hope, A. G., and Barnes, N. M. (2001) *Neuropharmacology 41*, 282−284.

23. Abraham, M. H., Grellier, P. L., Prior, D. V., Duce, P. P., Morris, J. J., and Taylor, P. J. (1989) *J. Chem. Soc.-Perkin Trans. 2*, 699−711.
24. Smart, B. E. (2001) *J. Fluor. Chem. 109*, 3−11.
25. Tonder, J. E., and Olesen, P. H. (2001) *Curr. Med. Chem. 8*, 651−674.
26. Schmitt, J. D. (2000) *Curr. Med. Chem. 7*, 749−800.
27. Tonder, J. E., Hansen, J. B., Begtrup, M., Pettersson, I., Rimvall, K., Christensen, B., Ehrbar, U., and Olesen, P. H. (1999) *J. Med. Chem. 42*, 4970−4980.
28. Sheridan, R. P., Nilakantan, R., Dixon, J. S., and Venkataraghavan, R. (1986) *J. Med. Chem. 29*, 899−906.
29. Curtis, L., Chiodini, F., Spang, J. E., Bertrand, S., Patt, J. T., Westera, G., and Bertrand, D. (2000) *Eur. J. Pharmacol. 393*, 155−163.
30. Kenakin, T. (2001) *FASEB J. 15*, 598−611.
31. Colquhoun, D. (1998) *Br. J. Pharmacol. 125*, 924−947.
32. Boess, F. G., Steward, L. J., Steele, J. A., Liu, D., Reid, J., Glencorse, T. A., and Martin, I. L. (1997) *Neuropharmacology 36*, 637−647.
33. Spier, A. D., and Lummis, S. C. (2000) *J Biol Chem 275*, 5620−5625.
34. Schmitt, J. D., Sharples, C. G., and Caldwell, W. S. (1999) *J. Med. Chem. 42*, 3066−3074.
35. Benowitz, N. L. (1996) *Annu. Rev. Pharmacol. Toxicol. 36*, 597−613.
36. Dani, J. A., and Heinemann, S. (1996) *Neuron 16*, 905−908.
37. McGehee, D. S., and Role, L. W. (1995) *Annu. Rev. Physiol. 57*, 521−546.
38. Jones, S., Sudweeks, S., and Yakel, J. L. (1999) *Trends Neurosci. 22*, 555−561.
39. Marubio, L. M., del Mar Arroyo-Jimenez, M., Cordero-Erausquin, M., Lena, C., Le Novere, N., de Kerchove d'Exaerde, A., Huchet, M., Damaj, M. I., and Changeux, J. P. (1999) *Nature 398*, 805−810.
40. Picciotto, M. R., Zoli, M., Rimondini, R., Lena, C., Marubio, L. M., Pich, E. M., Fuxe, K., and Changeux, J. P. (1998) *Nature 391*, 173−177.
41. Lena, C., and Changeux, J. P. (1997) *Curr. Opin. Neurobiol. 7*, 674−682.
42. Xie, Y., and Cohen, J. B. (2001) *J. Biol. Chem. 276*, 2417−2426.
43. Chiara, D. C., Middleton, R. E., and Cohen, J. B. (1998) *FEBS Lett. 423*, 223−226.
44. Seeman, J. I., and Whidby, J. F. (1976) *J. Org. Chem. 41*, 3824−8326.
45. Li, L. T., Zhong, W. G., Zacharias, N., Gibbs, C., Lester, H. A., and Dougherty, D. A. (2001) *Chem. Biol. 8*, 47−58.

BI020266D